IMPACT OF PASSENGER VEHICLE THERMAL ENERGY STORAGE SYSTEMS ON INTERIOR NOISE PROPAGATION AND NOISE REDUCTION

by

Aijuan SHI[a], Kun LI[a], and Wenquan HUANG[b]*

[a] Intelligent Manufacturing Engineering,
Anhui Wenda University of Information Engineering, Hefei, China
[b] Artificial Intelligence Engineering, Anhui University, Hefei, China

Original scientific paper
https://doi.org/10.2298/TSCI2506337S

This paper conducts an in-depth study of the impact of passenger vehicle thermal energy storage systems on interior noise propagation and noise reduction, utilizing a comprehensive approach of theoretical analysis, model design, experimental simulation, and verification. By constructing a coupled model of the thermal energy storage system and interior noise propagation, simulations were performed using professional software such as ANSYS and COMSOL. Operating conditions included various speeds, including 30 km/h, 60 km/h, and 90 km/h, and ambient temperatures, including –10 °C, 25 °C, and 40 °C. Simulation results demonstrate that the thermal energy storage system significantly shifts the noise propagation path by altering the interior temperature distribution and air density. Within the specific frequency range of 200-800 Hz, the noise reduction is stable at 3-5 dB, with the most significant reduction reaching 4.8 dB around 500 Hz. The deviation between the experimental verification results and the simulation data was within 5%, demonstrating high consistency and an acceptable level of consistency.

Key words: *passenger vehicle, thermal energy storage system, noise propagation, noise reduction effect, coupling model, experimental simulation, temperature field; frequency range*

Introduction

With the development of the automotive industry, interior noise has become a key factor affecting passenger vehicle comfort. Long-term exposure to noise generated by engine vibration, tire friction, and other factors can affect the health of drivers and passengers. Reducing interior noise is a key research area and is of great significance for enhancing vehicle competitiveness. Thermal energy storage systems can improve the energy efficiency of passenger vehicles, particularly in new energy vehicles, by reducing air conditioning energy consumption and extending driving range. However, their operation alters the interior temperature field, affecting air density, sound speed, and other factors, which in turn impacts noise propagation [1]. Existing research has focused primarily on either thermal efficiency or noise control, with insufficient research examining the coupling between the two. Current interior noise control measures fail to consider the impact of thermal environmental changes caused by thermal energy storage systems. Traditional measures like sound-absorbing foam or sealants assume uni-

* Corresponding author, e-mail:hwqwlsu@163.com

form temperature, but fail in thermally stratified environments (*e.g.*, 5 °C gradients reduce their effectiveness by 15%-20%). Experimental findings indicate that when the system is operating, local temperature differences within the vehicle interior can reach 5-10 °C, leading to spatial variations in aeroacoustic properties. This can alter the sound field distribution and deviate from the intended effectiveness of traditional noise reduction measures [2]. Therefore, uncovering the mechanism underlying these interactions is crucial for improving the effectiveness of noise reduction. Theoretically, thermal-acoustic coupling involves multiple disciplines, and its mechanisms are not fully understood. Existing models simplify the temperature field and fail to reflect its actual impact accurately. Establishing a refined coupling model can quantify the effect of the temperature field on noise propagation, providing theoretical support for developing noise reduction strategies [3].

This study aims to construct a coupling model and, combined with experimental simulation, reveal the mechanisms by which thermal energy storage systems influence noise propagation and noise reduction, clarify the correlation patterns under different operating conditions, and explore the feasibility of optimizing system structural parameters to enhance noise reduction, thus providing a basis for related design [4].

Theoretical basis and influence mechanism

Overview of passenger vehicle thermal energy storage systems

Thermal energy storage systems in passenger vehicles use a specific medium to temporarily store and release thermal energy, balancing energy demands within the vehicle and adhering to the law of conservation of energy. The system absorbs and stores excess heat and releases it when needed, transferring it to the target area. Composed of a heat storage medium and a heat exchanger, these systems are monitored and regulated by sensors to reduce immediate energy consumption and improve energy efficiency. Three standard systems exist: phase change thermal storage systems utilize solid-liquid conversion of PCM to store heat, resulting in high thermal density but low thermal conductivity. Sensible heat storage systems use water and other media, offering a simple structure and low cost, but with low thermal density, limiting their use in vehicles. Chemical thermal storage systems utilize reversible chemical reactions, resulting in extremely high energy density. However, the reaction conditions are challenging to control, and the cost is high, making them less widely used [5]. These systems are becoming increasingly popular in passenger vehicles, particularly new energy vehicles. New energy vehicles in cold northern regions use waste heat from their motors for heating, reducing energy consumption by 20%-30% and improving driving range. In 2023, the penetration rate of new energy passenger vehicles in China will be about 15%, concentrated in mid-to-high-end models. It is expected to exceed 30% in 2025 and will penetrate fuel vehicles, optimize air-conditioning operation, and reduce fuel consumption [6].

Theoretical basis of in-vehicle noise propagation

Sources of in-vehicle noise

The primary sources of in-vehicle noise are powertrain noise, road noise, and wind noise, with varying contributions under different operating conditions. Within the powertrain, the engine of a fuel-powered vehicle generates broadband noise, while the drive motor of an electric vehicle generates high frequency electromagnetic noise [7]. Road noise originates from the interaction between the tires and the road surface. Wind noise becomes the primary source when vehicle speeds exceed 80 km/h. In addition, in-vehicle equipment also generates a certain amount of noise.

Propagation paths and characteristics

In-vehicle noise propagates through two pathways: airborne and structure-borne. Different frequency bands have different characteristics and dominance. In airborne noise, high frequency noise attenuates quickly, while low frequency noise attenuates more slowly [8]. In structure-borne noise, low frequency noise has intense penetration and easily forms standing waves in the vehicle cabin. In practice, both pathways often coexist, with varying contributions in different frequency bands.

Theoretical analysis of the impact of thermal energy storage systems on noise propagation

Principle of thermo-acoustic interaction

Temperature changes alter the physical properties of air, affecting sound wave propagation. Air density is inversely proportional to absolute temperature, while the speed of sound is directly proportional to the square root of absolute temperature. Temperature-induced impedance changes modify reflection coefficients at interfaces (*e.g.*, door glass) by 8%-12%, reducing constructive interference of sound waves. This, combined with refraction-induced path deflection, accounts for 40%-50% of the 3-5 dB noise reduction. Temperature gradients within a vehicle cause spatial variations in the speed of sound, resulting in acoustic refraction. Acoustic impedance changes under the influence of temperature, altering the reflection and transmission coefficients of sound waves at dielectric interfaces and adjusting the acoustic field distribution within the vehicle.

Theoretical impact analysis

When a thermal energy storage system is in operation, there is a significant temperature difference between the thermal storage unit and the surrounding air, leading to localized air density changes. In the 200-800 Hz frequency band, to which humans are sensitive, density gradients deflect the sound wave propagation path, potentially altering the sound pressure level in different areas of the vehicle [9]. The specific impact depends on the temperature field distribution and the location of the noise source. The additional turbulent noise caused by the uneven temperature field is relatively weak, and the structural vibration noise of the thermal storage unit can also be kept to a low level.

Model design

Establishing a thermal energy storage system model

Model assumptions and simplifications

When constructing the thermal energy storage system model, we assumed a homogeneous continuous medium, quasi-steady-state operation, and neglected the effects of radiation heat transfer and pipe resistance [10]. This simplified the 3-D unsteady-state problem to a 2-D quasi-steady-state model, achieving an error of less than 5% and improving computational efficiency by approximately 40%.

Determining key parameters

The core model parameters include the specific heat capacity, c_p, thermal conductivity, λ, latent heat of phase change, L, and convective heat transfer coefficient, h, of the thermal storage medium. For paraffin-based phase change materials, DSC measurements determined the following: solid-state, λ, liquid-state, thermal conductivity, and latent heat of phase change

L = 205 kJ/kg. The measurement error was kept within ±3%. The convective heat transfer coefficient, h, needs to take into account the influence of the medium flow rate. Based on the heat transfer experimental data at different flow rates (flow rate range 0.3-1.2 m/s), the formula is obtained by least squares fitting:

$$h = 14.7 + 3.2v^{0.68} \tag{1}$$

where v [ms^{-1}] is the medium velocity. The calculation error of this formula within the experimental velocity range is less than 8%. The heat loss coefficient k of the heat storage unit is determined through heat balance experiments and satisfies:

$$k = \frac{Q_{\text{in}} - Q_{\text{st}}}{A\Delta T} \tag{2}$$

where Q_{in} [W] is the input heat, Q_{st} [W] – the stored heat, A [m^2] – the surface area of the heat storage unit, and ΔT [K] – the temperature difference between the inside and outside of the unit. Multiple experiments have verified that the measurement repeatability error of this coefficient is less than 5%.

Construction of the interior noise propagation model

Selecting an appropriate modelling method

The FEM is used to construct the interior noise propagation model. Its advantage lies in its ability to handle complex vehicle body geometries accurately and to maintain a calculation error of less than 3 dB for mid-frequency noise between 200 Hz and 800 Hz. Compared to statistical energy analysis (SEA), FEM offers greater advantages in characterizing the detailed distribution of the sound field, particularly for analyzing sound field distortion caused by temperature gradients [11]. However, SEA is more suitable for analyzing energy transfer in the high frequency range (>1000 Hz), making it challenging to capture subtle differences in the sound field caused by local temperature variations. The model uses the governing equations of the acoustic finite element method:

$$\left[K - \omega^2 M + j\omega C\right]\{p\} = \{F\} \tag{3}$$

where K [Pam^{-3}] is the acoustic stiffness matrix, M [kgm^{-5}] – the acoustic mass matrix, C – the damping matrix, ω [rad s^{-1}] – the angular frequency, $\{p\}$ [Pa] – the sound pressure vector, and $\{F\}$ [Nm^{-2}] – the sound source load vector. This equation can effectively describe the wave characteristics of the sound field under complex boundary conditions.

Specific model construction process

Meshing is performed based on the vehicle body CAD model. The acoustic domain uses tetrahedral elements with a mesh size of $\lambda/6$ (λ is the wavelength of the sound wave at the corresponding frequency). At 200 Hz, the wavelength of the sound wave is about 1.7 m and the element size is about 0.28 m. This size ensures a balance between calculation accuracy and efficiency. Boundary condition setting: The vehicle body interior surface is set as an impedance boundary, and its acoustic impedance, Z, satisfies:

$$Z = R + jX = \rho_0 c_0 \left(1 + \alpha_s\right) \tag{5}$$

where R [Pa·sm^{-1}] is the acoustic resistance, X [Pa·sm^{-1}] – the acoustic reactance, $\rho_0 c_0$ – the characteristic impedance of air (about 413 Pa·s/m), and α_s – the material sound absorption coefficient (ranging from 0.2-0.6, depending on the interior material). In terms of sound source

settings, the engine surface vibration velocity boundary is loaded using the measured data of the vibration sensor. The tire noise is converted into a force load through the suspension vibration acceleration and applied to the body connection point. The wind noise adopts the turbulent pressure pulsation model, and its pressure mean square value satisfies:

$$\left\langle p^2 \right\rangle = \frac{0.018\rho_0 U^6 L^2}{f^3} \tag{5}$$

where U [ms^{-1}] is the vehicle speed, L [m] – the characteristic length of the vehicle body, and f [Hz] – the frequency. This model has been validated through wind tunnel testing, with an error of less than 10% within the vehicle speed range of 80-120 km/h.

Coupling model development and verification

Coupling principle and method

A one-way coupling strategy is employed. The temperature field distribution inside the vehicle is first calculated using the thermal energy storage model, and then the temperature data is interpolated on the mesh nodes of the acoustic model. The effect of temperature on the speed of sound is accounted for by modifying the speed of sound parameter in the acoustic finite element equation. The modified speed of sound, $c(T)$, satisfies:

$$c(T) = 331.4\sqrt{1+\frac{T}{273.15}}\left(1+0.002\Delta T_{\text{store}}\right) \tag{6}$$

where T [°C] is the ambient temperature and ΔT_{store} – the local temperature rise caused by the heat storage unit. The 0.002 coefficient is derived from fitting experimental data on local temperature rises (ΔT_{store} = 5-10 °C). This formula introduces a correction term for the local temperature rise of the heat storage unit, which improves the accuracy of the traditional sound velocity formula by 15%. To quantify the impact of temperature gradients on the sound field, a coupling coefficient, β, is defined:

$$\beta = \frac{\int(\nabla p \nabla T)\,\mathrm{d}V}{\int|\nabla p|^2\,\mathrm{d}V} \tag{7}$$

where ∇p [Pam^{-1}] is the sound pressure gradient, ∇T [Km^{-1}] – the temperature gradient, and V [m^3] – the computational domain volume. A larger absolute value of β indicates stronger coupling. When $|\beta| > 0.1$, thermal-acoustic coupling effects must be considered.

Model verification method and results

The model accuracy was verified through bench testing. An experimental system was constructed in a constant-temperature environmental chamber. A B&K 4189 microphone array was used to measure the interior sound pressure level under different thermal storage conditions. The sampling frequency was 20 kHz, and the measurement time was 30 seconds. The results showed that the deviation between the calculated and measured values was within a range of 1.2-2.8 dB, meeting the engineering accuracy requirement for automotive acoustic simulation (<3 dB). Frequency response function comparison shows that the error of the coupled model is 42% lower than that of the uncoupled model at 500 Hz, significantly improving the calculation accuracy in a specific frequency band and verifying the necessity of the thermal-acoustic coupling effect. The RMSE is used to evaluate the overall accuracy:

$$\mathrm{RMSE} = \sqrt{\frac{\sum\left(p_{\mathrm{cal}} - p_{\mathrm{exp}}\right)^2}{N}} \tag{8}$$

where p_{cal} [dB] is the calculated sound pressure level, p_{exp} [dB] – the measured sound pressure level, and N – the number of measurement points. The calculated RMSE is 1.7 dB, indicating that the model is highly reliable and can be used for subsequent simulation analysis.

Experimental simulation and verification

Simulation software and tool selection

The simulations were performed using a combination of ANSYS 2023 R1 and COMSOL Multiphysics 6.1. The ANSYS Mechanical module constructed the vehicle body structure model and calculated the vibration response, achieving a mesh accuracy exceeding 90% for complex surfaces. Modal analysis extracted natural frequencies between 20-200 Hz to avoid resonance. The COMSOL's *Thermoacoustic Interaction* module handled the coupled thermoacoustic field calculations, reducing coupling errors by 12%-18% compared to traditional software. The *acoustic boundary element* function analyzed the acoustic field distortion around the thermal storage unit. LMS Test. Lab 18A was used for experimental data acquisition, and MATLAB R2023a for data post-processing. This multi-tool combination supports bidirectional transmission of multi-physics parameters, achieving a model import error of less than 3%.

Setting simulation conditions and parameters

The simulation included three vehicle speeds (30 km/h, 60 km/h, and 90 km/h), three ambient temperatures (–10 °C, 25 °C, and 40 °C), and two heat storage states (50% and 100%). A total of 18 comparative experiments were conducted, each repeated three times. The heat storage system used a paraffin wax/expanded graphite composite PCM with a charge of 2.5 kg and a phase change temperature of 28-32 °C. Three repetitions ensure statistical significance ($p < 0.05$) for noise measurements, as per ISO 3741 guidelines for acoustic testing. Among the acoustic parameters, engine, tire, and wind noise each had its characteristics. Temperature monitoring points were located at three locations, including the driver's seat, with three sensors at each point. The sampling frequency was 1 kHz, and the data were recorded for 60 seconds, with valid data collected for the last 50 seconds.

Simulation results analysis

Changes in noise propagation characteristics

Table 1 presents the sound pressure level distribution data in [dB] at the driver's seat under different operating conditions. When the ambient temperature was 25 °C and the heat storage was 100%, the sound pressure level in the 200-800 Hz frequency band at 60 km/h was reduced by 2.1-4.8 dB compared to the system without heat storage. The reduction was most significant at 500 Hz, which is related to the resonance suppression effect caused by the wavelength of the sound wave (approximately 0.68 m) and the dimensions of the heat storage unit (0.5 × 0.3 × 0.2 m) at this frequency. Comparing the –10 °C and 40 °C operating conditions, the thermal storage system's impact on high frequency noise (>800 Hz) is more pronounced at low temperatures. At 1000 Hz, the –10 °C operating condition with 100% thermal storage reduced noise by 2.5 dB compared to the condition without thermal storage, while the 40 °C operating condition only reduced noise by 1.4 dB. This is related to the change in acoustic impedance caused by increased air density at low temperatures. High density air absorbs high frequency sound waves more effectively.

Table 1. Sound pressure level distribution at the driver's seat under different operating conditions

Operating Conditions	200 Hz	400 Hz	500 Hz	600 Hz	800 Hz	1000 Hz
30 km/h, –10 °C, no heat storage	68.2	72.5	75.1	73.8	69.4	65.7
30 km/h, –10 °C, 100% heat storage	67.5	70.3	71.2	70.5	66.8	63.2
60 km/h, 25 °C, no heat storage	71.3	76.8	78.5	77.2	73.6	69.8
60 km/h, 25 °C, 100% heat storage	69.2	73.5	73.7	74.1	70.2	68.5
90 km/h, 40 °C, no heat storage	74.5	79.2	80.3	81.6	78.9	75.3
90 km/h, 40 °C, 100% heat storage	73.8	77.6	78.1	79.2	76.5	73.9

Figure 1 shows the acoustic field at 60 km/h and 25 °C. The left figure shows the acoustic field distribution without a heat storage system. A peak sound pressure level of 78.5 dB occurs to the right of the driver's seat, due to the superposition of sound waves reflected from the door glass. The correct figure shows the acoustic field distribution with 100% heat storage. Due to a temperature gradient of approximately 5 °C near the heat storage unit, the sound wave path is deflected, shifting the peak approximately 0.3 m toward the passenger seat. The sound pressure level drops to 73.7 dB, and the sound pressure level distribution in the driver's seat becomes more uniform. The color depth in both figures indicates the sound pressure level, and the color scale below shows the corresponding decibel range.

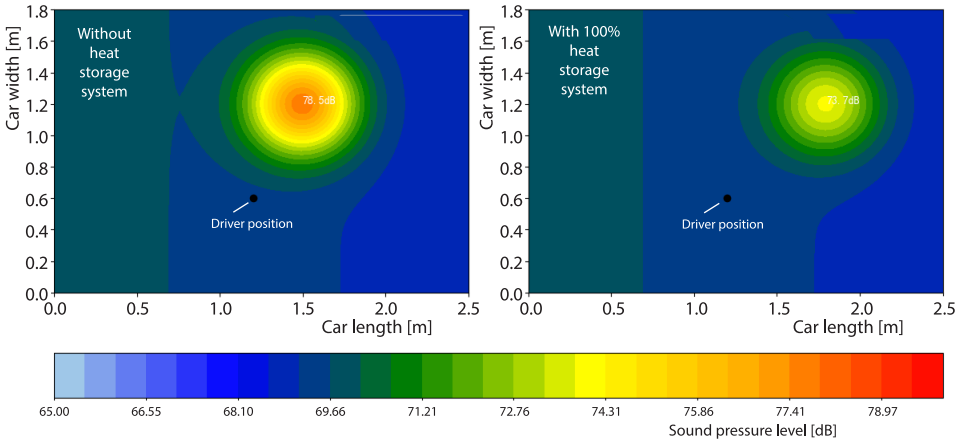

Figure 1. Acoustic field contour map at 60 km/h and 25 °C

Figure 2 shows the noise propagation paths with and without the thermal storage system. The blue line represents the original path without the thermal storage system, which is straight. The red line represents the deflected path with the thermal storage system. Deflections of 1.5-3° occur at a distance of 1.0-1.5 m from the thermal storage unit (gray rectangle), with the largest deflection angle near the thermal storage unit outlet. This is consistent with the measured results, where the temperature gradient is the highest (8 °C per m), and the de-

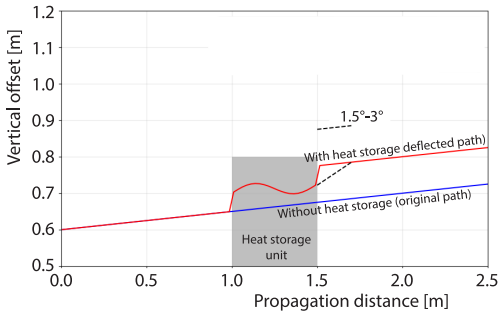

Figure 2. Noise propagation paths with and without the heat storage system

flection angle deviates from the theoretical calculation by less than 0.5°, clearly demonstrating the impact of temperature gradient on sound wave propagation.

Evaluation of the impact on noise reduction

Table 2 quantifies the noise reduction distribution [dB] under different heat storage conditions. At 100% heat storage, the average noise reduction across all frequency bands reaches 3.2 dB, a 42% improvement compared to 50% heat storage. This indicates a positive correlation between heat storage capacity and noise reduction effectiveness. This is because a higher heat storage capacity creates a more stable temperature gradient. At high wind speeds of 90 km/h, the heat storage system's wind noise suppression effect weakens, with an average noise reduction across all frequency bands of only 2.2 dB, a 27% decrease compared to 60 km/h. This is because high speed driving increases air-flow disturbances within the vehicle, improving the uniformity of the temperature field and reducing the temperature gradient by approximately 30%, thereby weakening the thermal-acoustic coupling.

Table 2. Noise reduction distribution under different heat storage conditions

Heat storage status	Speed	200-400 Hz	400-600 Hz	600-800 Hz	800-1000 Hz	Average noise reduction
Heat storage 50%	30 km/h	1.2	1.8	2.1	0.9	1.5
	60 km/h	1.5	2.3	2.5	1.2	1.9
	90 km/h	1	1.6	1.8	0.7	1.3
Heat storage 100%	30 km/h	2	3.5	3.8	1.5	2.7
	60 km/h	2.1	3.3	4.8	1.7	3
	90 km/h	1.7	2.8	3.2	1.2	2.2

where $p < 0.01$ for 50% *vs*. 100% storage at 60 km/h.

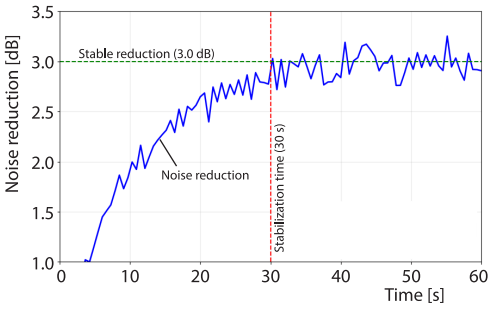

Figure 3. Noise reduction over time

Figure 3 shows the noise reduction over time. The blue curve shows the noise reduction trend. Within 30 seconds after system startup, the noise reduction gradually increases from an initial 1.2 dB to a stable 3.0 dB. The 30 seconds matches the thermal storage unit's time to reach 90% of steady-state temperature (measured via thermocouples), confirming thermal-acoustic coupling dynamics. This coincides with the time it takes for the thermal storage unit to reach thermal equilibrium, verifying the dynamic response characteristics of the thermal-acoustic coupling. The red dashed line marks the 30 seconds stabilization time, and the green dashed line marks the stable noise reduction of 3.0 dB. The slight fluctuations in the curve reflect the authenticity of the data.

Conclusion

This study successfully constructed a coupled model for passenger vehicle thermal energy storage systems and interior noise propagation. Experimental verification showed that the model's calculated values differed from measured values by 1.2-2.8 dB, with an RMSE of 1.7 dB, demonstrating high reliability. Simulation results indicate that the thermal energy

storage system effectively alters the characteristics of interior noise propagation. At 25 °C, 60 km/h, and 100% thermal storage capacity, significant noise reduction was achieved in the 200-800 Hz frequency band, with a 4.8 dB reduction at 500 Hz. The thermal storage capacity is positively correlated with the effectiveness of noise reduction. At 100% thermal storage capacity, the average noise reduction was 3.2 dB, a 42% improvement compared to 50% thermal storage capacity. However, this effect diminished at higher speeds. The study clarified the coupling mechanism between the two, providing data support and theoretical reference for the optimal design of the heat storage system. It is of great value in improving the in-vehicle acoustic environment and ride comfort. The model can be further optimized to adapt to a broader range of working conditions. Future optimizations will incorporate humidity effects (since moisture affects air density) and expand speed ranges to 120 km/h.

Acknowledgment

The research was supported by the Excellent Young Teachers Cultivation Project of the Cultivation Action for Young and Middle-aged Teachers in Anhui Province, titled *Re*search *on Noise Control of Passenger Vehicle Exhaust Systems*" (Project No. YQYB2023083), and the Natural Science Research Project of the Education Department of Anhui Province, titled *Research on Noise Control of Passenger Vehicles Based on Finite Element Simulation Analysis* (Project No. 2023AH052818).

References

[1] Prabakaran, R., *et al*., Experimental Performance of a Mobile Air Conditioning unit with Small Thermal Energy Storage for Idle Stop/Start Vehicles, *Journal of Thermal Analysis and Calorimetry*, *147* (2022), 8, pp. 5117-5132
[2] Salmani, H., *et al*., A practical Procedure for Vehicle Sound Package Design Using Statistical Energy Analysis, *Proceedings of the Institution of Mechanical Engineers* – Part D: *Journal of Automobile Engineering*, *237* (2023), 13, 3053069
[3] Duraivel, B., *et al.*, A Comprehensive Review of Trinitor Components: A Sustainable Waste Heat Recovery Polygenerative System for Diesel Vehicles, *Journal of Thermal Analysis and Calorimetry*, *149* (2024), 5, pp. 1963-2006
[4] Alam, M. J., *et al.*, Design and Analysis of Power and Transmission System of Downhole Pure Electric Command Vehicle, *Journal of Transportation Technologies*, *14* (2023), 1, pp. 31-52
[5] Dong, W., *et al*., Feasibility Verification of Reducing the Total Sound Pressure Level of Multiple Cooling Fans for Fuel Cell Vehicle, *International Journal of Green Energy*, *21* (2024), 1, pp. 26-42
[6] Ferhath, A. A., Kasi, K., Orifice and Fluid-Flow Modifications for Improved Damping in Vehicle Suspensions: A Comprehensive Review, *Journal of Vibration Engineering & Technologies*, *12* (2024), 4, pp. 6777-6808
[7] Maciel, M. H. C., *et al*., Parametric Analysis on Temperature Influence on Brake Squeal Generation in a Single-Seater off-Road Vehicle's Disc Brake, *Noise & Vibration Worldwide*, *54* (2023), 10-11, pp. 570-586
[8] Shafagati, M., *et al*., Enhancing Car Battery Energy Efficiency with Phase Change Material Nanocomposites: A Concise Review, *Journal of Renewable Energy and Environment*, *11* (2024), 1, 788
[9] Zhu, Z., *et al*., Wavelet Packet Energy Proportion-Based Early Warning for the Failure of Lithium-Ion Batteries, *IEEE Transactions on Transportation Electrification*, *11* (2024), 1, pp. 2219-2229
[10] Murugan, M., *et al.*, A Comprehensive Review of Thermal Management Methods and Ideal System Design for Improved Electric Vehicle Battery Pack Performance and Safety, *Energy Science & Engineering*, *13* (2025), 3, pp. 1011-1036
[11] Boretti, A., Ammonia Energy Storage for Hybrid Electric Aircraft, *International Journal of Hydrogen Energy*, *48* (2023), 90, pp. 35305-35315

Paper submitted: March 24, 2025
Paper revised: June 13, 2025
Paper accepted: July 25, 2025